Response characteristics in the lateral geniculate nucleus (LGN) and their primary afferent influences on the visual cortex of cat

Florentin Wörgötter*, Katrin Suder† and Klaus Funke†

* University of Stirling, Department of Psychology, Stirling, FK9 4LA, Scotland, UK

Phone: +44-1786-466369 FAX: +44-1786-467641

Email: worgott@cn.stir.ac.uk

† Institute of Physiology, Department of Neurophysiology, Ruhr-University, Universitätsstrasse 150, D-44780 Bochum, Germany

Phone: +49-234-322-4940 FAX: +49-234-321-4192

Email: funke@neurop.ruhr-uni-bochum.de

Stirling, 8th November 2000

Abstract

In this article, which bears to a large degree review character, we first summarize the connection structure of the LGN and how it is embedded into the primary visual pathway. We continue describing its basic physiological properties focusing on inhibitory influences which contribute to the (non-)linearity of the LGN cells. The sections on the LGN are concluded with a description of its dynamic response properties and how LGN cells change their behavior during different EEG states. This type of behavior is then traced into the visual cortex where receptive fields change in a state dependent way. In addition, one finds that the receptive field size shrinks during the first few hundred milliseconds of continuous stimulation. The last part of this chapter is therefore devoted to a neural field model which tries to explain the cortical receptive field shrinkage in a mathematical way. Intriguingly the model claims that cortical receptive field shrinkage does not require intracortical interactions but seems to be a process entirely dominated by the dynamic structure of the LGN activity described in the first part of this article.

1 Introduction

The primary visual pathway consists of three substructures: retina, lateral geniculate nucleus (LGN), which is a part of the thalamus, and the visual cortex with its many different areas. All these structures are connected by

afferent fibers and the hierarchical arrangement, which dominates the first levels, is given up at the level of the cortex, where it is replaced by a widely branching parallel connectivity. Apart from the retina, rich feedback connections exist between cortex and thalamus as well as lateral connections between the different cortical areas. These anatomical observations, for which strong evidence accumulated not later than around 1970 [7, 46, 48, 60], indicate that visual information processing must be a process utilizing recurrent loops and involving massive dynamic interactions.

In addition, it can be observed that the visual world at the level of a single LGN or cortical cell (outside an electrophysiology laboratory) is anything but predictable. Receptive fields (RFs) very often encounter new stimulus situations due to fast (saccadic) eye movements, which occur at an average rate of 3/s, and/or due to object motion in the viewed scene. All this can be interpreted as a constantly changing flow of information which enters the visual system. The network has to react to these changes in order to create a reliable visual perception. As the direct consequence of the fast changing signals which arrive at any given cell a strongly varying activity pattern is observed as its output. Through lateral and feed-back connectivity this activity re-enters the cortical network at all levels and is able to influence even those cells (and especially their receptive field structure) from which it initially originated.

In this review article we will first concentrate on the LGN and first describe the basic properties of its cells and the known features of their connectivity which lead to these responses. Then, we will show that the response characteristics of thalamic and cortical cells can change rather strongly in a way correlated with the global state of the brain as measured by electroencephalographic activity (EEG). Here, we will compare changes of the temporal response pattern of thalamic cells with those of the mean impulse rate and also with temporal and spatial changes of cortical response fields (receptive fields). We will then continue with a neural field model that can explain the temporal restructuring of cortical receptive fields on the basis of changes of the temporal characteristics of thalamic responses.

2 Experimental Findings

2.1 The LGN circuitry

The complex connectivity of the LGN is schematically shown by the wiring diagram of figure 1. The main vertical stream originating in retinal ganglion cells goes via LGN relay cells to the primary visual cortex. Only a small fraction (10-15%) of the synapses on LGN relay cells are of retinal origin, about 20% can be related to local inhibitory circuits including the peri-geniculate nucleus (PGN) and the remainder is made by excitatory feedback from the visual cortex (about 40%)and by diverse visual and non-visual

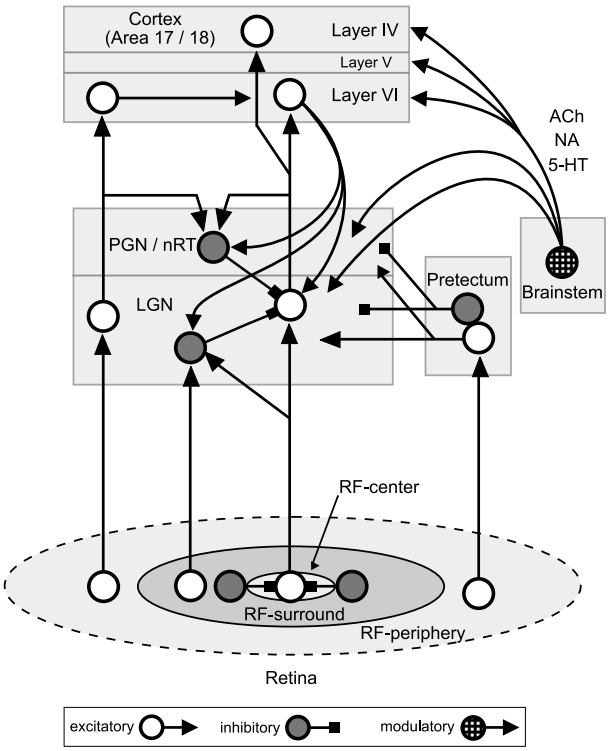

Figure 1: *Wiring diagram of LGN connectivity*

pathways originating in different brain stem structures. The brain stem connections use several different transmitters (acetylcholine, noradrenaline, serotonin, dopamine, GABA and glutamate) and are summarized as so called "modulatory inputs". Corticofugal and modulatory projections also terminate on local LGN interneurons and PGN neurons. Actually, the primary visual pathway consist of at least 4 parallel channels, the On- and Off-pathway and the parvo-(X) and magno-cellular (Y) pathway, which originate in the retina and have been shown to interact at the LGN in an inhibitory fashion. Within the LGN about 20-25% of the neurons are local inhibitory (GABAergic) interneurons. They also receive direct retinal input and project to LGN

relay cells (feedforward inhibition). Their axons do not leave the nucleus and probably do not cross the layers (A, A1, C) of the LGN [60]. A second source of inhibition at thalamic level emerges from the neurons of the perigeniculate nucleus (PGN) which is a part of the thalamic reticular nucleus (TRN) and joins the dorsolateral aspect of the LGN. The PGN neurons receive direct input from axon collaterals of LGN relay cells and, thereby, a negative feedback loop is established.

2.2 Physiological Properties of the LGN

2.2.1 Organization of Receptive Fields

The spatial characteristics of LGN RFs are very similar to their retinal counterparts. They are almost circular in shape and are composed of an excitatory center and an antagonistic (inhibitory) surround [35, 30]. Therefore, the LGN was first seen as an "internal retina". Actually, the LGN is more than a spatial copy of the retina as will be shown in the following. In mathematical terms the RF can be described as a combination of two centered gaussian sensitivity profiles of opposite polarity (the excitatory center and the antagonistic surround; [42], see figure 2A,C). The summation of both profiles results in a "mexican hat-like" structure, the basis for a spatial luminance filter. If the size of a spot of light flashed in the center of the RF is stepwise increased, the response of the neurons first increases and then steadily decreases when the spot extends beyond the center-surround border. Y and X

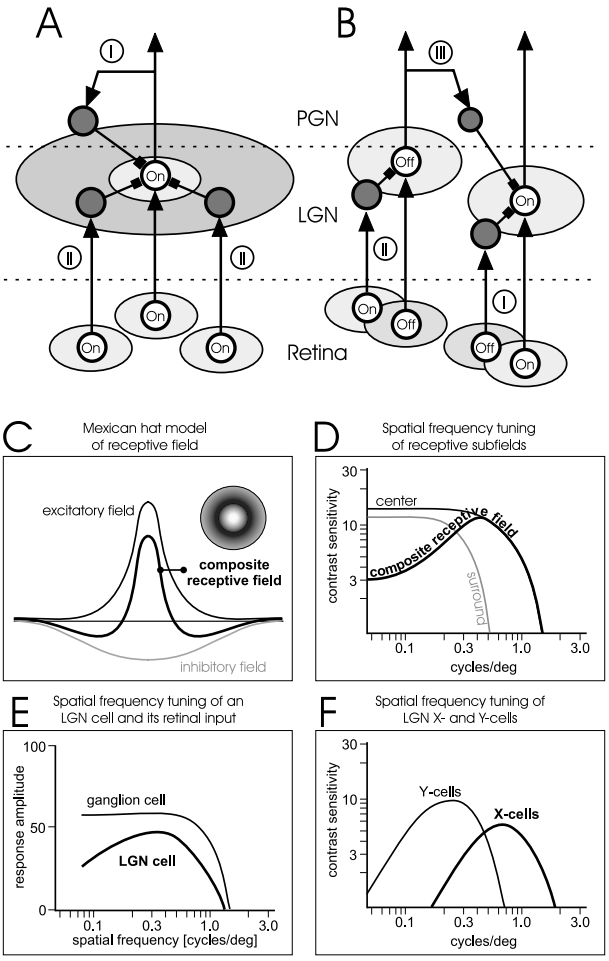

Figure 2: *Excitatory and inhibitory influences on the LGN (A,B) and the resulting shape of the receptive field (C) and its contrast sensitivity (D-F) A) Synergistic inhibition is either a feedback inhibition within the same channel (On or Off, pathway I), or a lateral interaction between inputs of the same RF-center type (On-On, pathway II). B) Reciprocal inhibition is an interaction between inputs of different RF-center type (On-Off, Off-On). Reciprocal inhibition is also possible via the PGN-loop (III). C) Composite RF of centered excitatory and inhibitory fields (Mexican-hat model, [42]). D) Contrast sensitivity functions of RF center surround and composite RF. E) Comparison of spatial frequency tuning of retinal ganglion and geniculate cells. F) Spatial frequency tuning in LGN X- and Y-cells.*

cells differ with respect to their RF size and contrast sensitivity (the relative illumination to background to which the system is adapted). The RFs of Y-

cells are about 3 times larger than those of X-cells and are therefore clearly more light-sensitive than X-cell RFs. In addition, the relative strength of the antagonistic RF surround seems to be weaker in Y-cells compared to X-cells.

2.2.2 Spatial Frequency Tuning

The spatial filter characteristic of the RF can be described by the contrast sensitivity function (CSF, Fig. 2D-F). Contrast sensitivity, the reciprocal of the contrast needed to elicit a criterion threshold response is plotted versus the spatial frequency of a test grating which is moved across the RF at optimal velocity. The peak of the resulting curve represents the optimal spatial frequency for the cell. Then, center and surround of the RF are stimulated by opposite contrasts of the grating and one half of the spatial cycle roughly corresponds to the RF center diameter. The curve shows a steep cutoff at higher spatial frequencies which results from a mixed coverage of RF center and surround by bright or dark bars. A decline in sensitivity is also found at lower spatial frequencies due to a stimulation of center and inhibitory surround. The spatial tuning curve of the complete RF can be predicted from the difference-of-gaussian (DOG) model based on the sensitivity profiles of RF center and surround (see [9] and figure 2B). A comparison of the spatial frequency tuning curves of ganglion cells and LGN relay cells demonstrates a stronger rolloff at low frequencies for the LGN cells (Fig. 2E) and can be explained by additional inhibitory surround mechanisms originating in

the LGN (see below). The optimal spatial frequency of cat X-cells close to area centralis is on average 1 cycle/degree, that of Y-cells around 0.3-0.5 cycles/degree (figure 2F). Due to some jitter in RF-diameter both classes build a continuum of spatial filters that coincides with the behavioral range of spatial frequency detection.

2.2.3 Synergistic Inhibition and Spatial Contrast

Visual processing in the LGN is dominated by inhibitory interactions of different kind which modify the spatial and temporal properties of the visual response. The so called "synergistic inhibition" evolves from inputs possessing the same RF type. For example, light On elicits an excitatory response within the RF center of an On-cell but also an inhibition mediated by the same cell or other On-cells. Two spatially different types of synergistic inhibition can be distinguished. One is carried by feedback inhibition within the center of the RF. On-center activity of an On-type ganglion cell drives an LGN On-cell. Thereafter, the LGN relay cell activates inhibitory neurons (local interneuron or PGN cell) and which project back to and inhibit the relay cell (pathway I in figure 2A). This inhibition of the recurrent type may cause the post-peak inhibitory response often visible between the early transient and the following tonic response of LGN relay cells. Feedback inhibition may serve to control the gain of the contrast-response relationship (which is generally lower in LGN compared with the retina) and modifies the tempo-

ral waveform of geniculocortical responses volleys [21]. The second type of synergistic inhibition acts as lateral inhibition (pathway II, figure 2A) and amplifies the center-surround antagonism [50]. LGN cells have been found to show a clearly stronger center-surround antagonism than retinal ganglion cells [30], an indication for an additional inhibitory surround evolving at the thalamic level. One clear difference between retinal and geniculate surround inhibition is that retinal surround inhibition fades with dark-adaptation but geniculate lateral inhibition does not. It has been suggested that this type of inhibition is of the feedforward type because lateral inhibition in the LGN has about the same latency as the excitatory center response and is mediated by direct inputs of surrounding ganglion cells to local geniculate interneurons (pathway II in figure 2A). The main function of the feedforward type of lateral inhibition is to enhance spatial (or simultaneous) contrast discrimination. A further, more wide-spread, inhibitory surround seems to emerge via recurrent inhibition: axon collaterals of neighboring LGN relay cells converge onto PGN neurons and elicit a volley of feedback inhibition as mentioned above. Due to the convergence of numerous LGN relay cells the PGN cells possess large RFs and are discussed to mediate the so called long-range lateral inhibition [17].

2.2.4 Reciprocal Inhibition and Successive Contrast

Reciprocal inhibition reflects the interaction of ganglion cell inputs with different center response type at LGN cells (see [49]). For example, an On-center ganglion cell directly excites an On-center LGN cell and an Off-center ganglion cell at the same retinal location inhibits the LGN cell via a local GABAergic interneuron (pathway I in figure 2B). In this way, an ON-type relay cell is excited by a bright stimulus projected into the center of its receptive field, but also actively inhibited by a dark stimulus or the offset of a bright stimulus. The opposite wiring scheme is valid for an Off-center LGN cell at any location within the LGN (pathway II in figure 2B). This so called "push-pull" mechanism increases and sharpens the response to a change in contrast, assures the linearity of responses and promotes successive contrast detection. Reciprocal inhibition seems to be mediated primarily by local interneurons in a feedforward manner, nevertheless, PGN cells receive convergent input from On- and Off-relay cells, so that a recurrent component could also contribute (pathway III in figure 2B). Inhibitory interactions of the push-pull type have been also postulated for the retinal network [24].

2.2.5 Binocular (inter-ocular) Inhibition

A third functional type of geniculate inhibition is characterized by the interaction of the two ocular channels which in other respects remain separate

at the subcortical level. Inter-ocular inhibition of an LGN relay cell is best visible when the so called "non-dominant eye" is visually stimulated while the dominant eye is closed to prevent a direct modulation of activity by excitatory inputs from this eye. Excitation in one eye is mediated via the corresponding LGN A-layer and further passed to the PGN. The feedback projection of the PGN to both A-layers results not only in an iso-ocular but also a cross-ocular (inter-ocular) feedback inhibition.

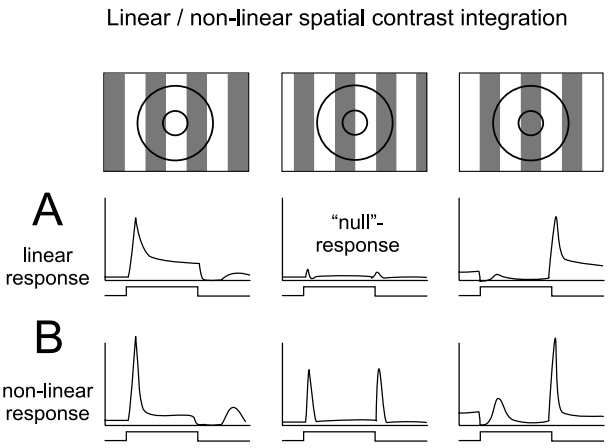

Figure 3: *Linear, X-type (A) and nonlinear, Y-type (B) spatial contrast integration. A) The strongest visual responses of the linear type are elicited in LGN X-cells by a contrast pattern of a spatial frequency that fits well to the diameter of the center of the RF. The strength of the visual response depends on the spatial phase of the pattern (e.g. a grating). A balanced stimulation of the RF center (and surround) by bright and dark bars results in the null-response (middle) which is characterized by only small, if any change in activity. B) Y-cell activity is more phasic and also characterized by the lack of a null-response. Non-linear (second order) response peaks are observed irrespective of the spatial frequency of the stimulus.*

2.2.6 Linear and Non-Linear Summation

The RF-composition described above is called the "linear summation field" of the RF. Linearity of spatial contrast integration is usually tested by flashing or counter-phasing (contrast reversal) a grating of optimal spatial frequency at different positions (spatial phases) with respect to the center of the RF [45]. The luminance of the grating is varied in a sinusoidal fashion. A bright bar centered on an On-cell RF with flanking dark bars covering parts of the surround causes a strong excitatory response. If the grating is reversed in contrast or shifted by 180°of spatial phase, the strongest inhibitory response is elicited. However, if the grating is shifted by 90°, both center and surround are covered by equal surface areas of bright and dark bars and excitatory and inhibitory responses are balanced. The result of a contrast reversal at this position is a "null-response" characterized by an almost absent modulation of activity (see figure 3A). This kind of behavior is typical for X-cells. Y-cells, however, show a somewhat different kind of contrast integration. At low spatial frequencies (optimal frequency, matched to RF center size) they also show an almost linear integration of contrast similar to X-cells. At higher spatial frequencies - exceeding the spatial resolution of their RF center - the linear response shows the typical cutoff and another type of response evolves: an excitatory response is elicited with each contrast reversal of the grating, resulting in 2 excitatory responses (one On and one Off response)

for each complete stimulus cycle (figure 3B). The cell now responds with a frequency twice that of the stimulus frequency. This so called second harmonic response is a non-linear kind of contrast integration suggested to be generated by the rectified (only excitation is passed) convergent activity of On- and Off-subunits which are smaller than the linear RF of the Y-cell but are of about the same size as the RF centers of X-cells. The non-linear input field seems to exceed the limits of the "classical" linear RF and also mediates the so called "periphery effect" or "shift-effect" [18].

2.2.7 Contrast Gain Control

Retinal and geniculate cells respond to increasing stimulus intensity (or contrast) with an almost proportional increase in firing rate, so that the relative stimulus intensity is represented by the mean firing rate. A contrast-response function can be established by plotting firing rate versus contrast on a logarithmic scale. A comparison of retinal and geniculate contrast-response functions reveals that the geniculate function is characterized by a smaller slope [32], indicating that contrast gain is reduced in the LGN. Intrageniculate inhibition of the feedback type (probably via the PGN) has been suggested as the fundamental mechanism. At a first view, this reduction in contrast gain is surprising because the lowered gain diminishes the resolution of contrast differences. However, it has to be considered that many LGN relay cells converge onto a cortex cell. One idea is that the reduced gain prevents

cortical cells from being overexcited and thereby loosing contrast resolution due to early saturation. The reduction of geniculate contrast gain should be compensated by the summation of multiple geniculate inputs at the cortical cell and as a positive side-effect, the influence of noise will be reduced. A temporally structured activity will further promote this effect as described below.

2.2.8 Response Latency

Several parameters, like the magnitude of change in stimulus intensity, the slope of the change, the size of the stimulus, the cell type and the temporal pattern of an input activity, can affect the latency of a visual response in retina, LGN and cortex (see [23]). Usually, response latency declines with increasing contrast and with increasing stimulus size. The higher the amount of light energy, which is collected by the receptive field of a ganglion cell, the stronger and steeper is the change of membrane potential and firing threshold is reached faster. Due to the effect of surround inhibition a large stimulus driving both the center and the surround of a RF elicits a smaller response amplitude than a stimulus confined to the center. Nevertheless, response latency may be shorter because surround inhibition is lagging behind the excitatory center response by a few milliseconds [16]. In addition, response latency exhibits some degree of variability even when identical stimuli are presented. Spontaneous fluctuations of the membrane potential (noise) may

be one reason for variable spike timing. The standard deviation of the latency declines with decreasing latency [5]. The minimal response latency of Y-cell responses is about 30 ms, that of X-cells is on average 10-15 ms longer. However, with suboptimal stimulation of the RF center by a small spot, response latency of a Y-cell can be longer than that of an X-cell. The response of ganglion cells precedes that of LGN relay cells by 2-4 ms. The intraretinal conduction velocity of ganglion cell axons is only 1.5-3.0 m/s because of the missing myelin shield. The myelinated part within the optic nerve has a considerable higher conduction velocity (30-50 m/s for Y-axons and 15-23 m/s for X-axons). Transmission of geniculate signals to cortex takes 2-5 ms with the Y-axons leading by 1-3 ms.

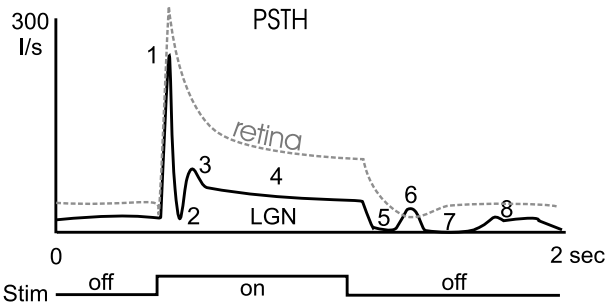

Figure 4: *Typical LGN cell responses. The peri-stimulus-time histogram (PSTH) on top shows a typical temporal waveform of a geniculate (thick line) and retinal (broken line) visual response to a light spot flashed on and off within the center of the receptive field. The response to a sudden increment and decrement of RF illumination can show up to 8 components:1) initial transient response (overshoot, peak), 2) post-peak inhibition, 3) early rebound response, 4) tonic response, 5) stimulus off inhibition (off-response), 6) first post-inhibitory rebound, 7) late inhibitory response, 8) second post-inhibitory rebound. The response profile of the retinal input is less complex.*

2.2.9 Response Dynamics

Depending on the temporal characteristics of the photopic input, the visual responses of retinal and geniculate projection cells show a distinct temporal waveform. For instance, a sinusoidal modulation of light intensity inside the receptive field is followed by an also almost sinusoidal change in firing frequency but with a phase difference which is depending on cell type and temporal frequency of the stimulus [28]. On the other hand, a steep increment (for On-cells) or decrement (for Off-cells) in light intensity in the RF center produces a bimodal response with an initial phasic response (overshoot) and a following tonic response. The latter slowly adapts during standing contrast mainly due to adaptation of photoreceptors and mechanisms intrinsic to retinal and LGN networks. A comparison of the response of an LGN cell with its afferent retinal input shows distinct differences (Fig. 4). First of all, the geniculate response is generally smaller than its retinal counterpart indicating a transfer ratio less than 100% [11, 12]. This transfer ratio can strongly change in a state-dependent way [12], a matter described later on in more detail. Below saturation level both response components (phasic and tonic) are almost equally reduced as revealed by a comparison of the phasic-tonic-index (PTI, the ratio of phasic to tonic firing frequency) of retinal and geniculate responses. The initial overshoot (1) of LGN responses is often followed by a transient drop in firing rate (2) below that of the follow-

ing tonic response, usually called "the post-peak-inhibition" which seems to evolve from intra- or perigeniculate inhibitory interactions. This inhibition is often followed by a "rebound" response (3) at the beginning of the tonic response (4). In addition, LGN cells also show a stronger decline in firing (5) when contrast changes in the direction opposite to RF center sensitivity (e.g. light Off for an On-center cell) which is the result of reciprocal inhibition (see above). This inhibitory Off-response also exhibits a multimodal time course. The strong and phasic inhibition after offset of stimulus is often followed by another rebound response (6) composed of a short burst of action potentials. The rebound is usually followed by a second inhibitory response (7) which is weaker and more sustained. Additional bursts of action potentials can occur during the declining phase of the inhibition with variable latency (8). These rebound burst are not of retinal origin, are intrinsically generated by the LGN relay cell and are the only period during which retino-geniculate transfer ratio is higher than 1.0. X- and Y-cells slightly differ in their response dynamics. Y-cells were often called "the phasic or transient cells" because they exhibit a stronger initial overshoot and a less prominent sustained tail of their response when compared to X-cells (tonic cells; see [6, 11]). So far, little is known about the significance of the different components of the visual response for higher level visual processing. The phasic and the tonic responses can be interpreted as two different messages about the visual stim-

ulus: the slope of an intensity change is primarily transmitted by the initial phasic response, whereas the tonic part of the response carries information about the steady contrast difference between the new and the former intensity [28]. Therefore, the phasic response might be used by the visual system to detect changes in the visual environment which are produced by fast eye or object motion. The tonic activity may be needed to analyse finer details like patterns and gradations in brightness and color.

2.3 The influence of the EEG-state on thalamic cell responses

2.3.1 EEG-effects in the LGN

The response characteristic of an LGN relay cell as shown in the PSTH of figure 4 is also influenced by the general level of excitability of the cell which, for example, is reduced during sleep [19, 46, 52]. Excitatory brain stem and corticofugal influences are diminished during an EEG state which is dominated by δ-waves [19, 48]. This state is in a non-anesthetized situation usually associated with deep sleep. In an anesthetized preparation still strong spontaneous transitions between a δ-wave dominated (so called synchronized EEG) and an EEG of reduced δ-wave activity (so called non-synchronized EEG) can be observed.

In Fig. 5 we show a few PSTHs of LGN cells recorded during synchronized and non-synchronized EEG. The same cell changes its firing charac-

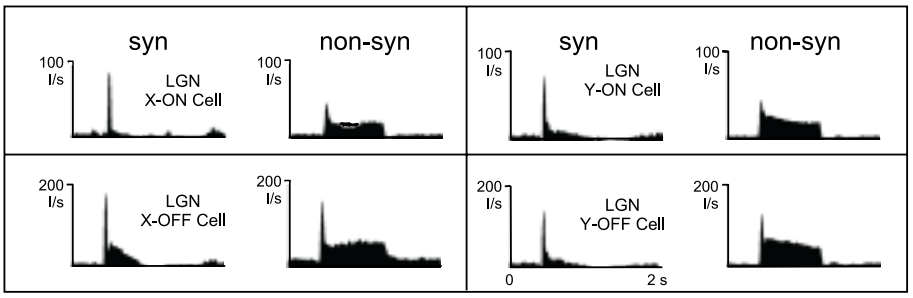

Figure 5: *PSTHs from four different LGN cells recorded during different EEG states. During synchronized EEG strong phasic bursts are observed at onset of the stimulus but tonic visual activity is strongly reduced. During non-synchronized EEG the initial bursts are often reduced in size and are followed by a pronounced tonic response.*

teristic completely when such an EEG transition happens. During a non-synchronized EEG, the initial phasic response is followed by a pronounced tonic response component which is almost missing during synchronized EEG. Such transitions can occur on a rather short time scale. Fig. 6 gives an example where two EEG-transitions (from non-syn. to syn. and back) occur within 200 seconds of recording time. The EEG traces on top (Fig. 6A) show that δ-waves are more pronounced between stimulus sweep 25 and 75 when tonic LGN light responses disappeared (Fig.6B). An additional observation can be made during an EEG change: Not only the shape of the PSTH but also the distribution of the inter-spike intervals changes. In this article we focus on response changes at the level of the PSTH because we will trace these changes into the cortex and derive a model to try to explain the results. Therefore we will not discuss observations which concern the inter-spike in-

terval distributions[1] and, instead, we refer the reader to the literature [22], for a review see [23]).

2.3.2 The LGN-PGN antagonism

The primary visual thalamus consists of the LGN and an accessory structure, the perigeniculate nucleus (PGN) which is a thin cell layer covering the LGN at its dorsolateral border. Anatomically the PGN is part of the thalamic reticular formation and functionally it is involved in the generation of EEG sleep-spindles [3, 33, 39, 44, 58] and - together with the corticofugal loop - also of δ-waves. LGN and PGN form a recurrent excitatory-inhibitory loop: LGN cells excite PGN cells and these in turn inhibit the LGN cells. Fig. 7 shows that this leads to a pronounced LGN-PGN antagonism. The LGN cell firing rate is reduced significantly as soon as the PGN cell fires strongly. This antagonism is also correlated with the state of the EEG (not shown). We have previously shown that increasing δ-activity of the EEG is associated with reduced LGN firing [36]. With simultaneous recordings of the activity of topographically matched PGN and LGN cells we could also demonstrate that PGN firing is usually increased during high EEG δ-

[1] Briefly: In general, many LGN cells (mostly of the On-type) show a multi-modal firing pattern, where the inter-spike interval histogram (INTH) consists of multiple, equidistantly spaced peaks. During reduced activity, such as that found when the EEG is δ-wave dominated, one must expect a reduced mean firing rate and thus, longer temporal intervals between two spikes. However, due to the quantal (multi-peak) character of these INTHs, intervals do not gradually lengthen, instead one observes that the number of short intervals diminishes (first peak gets smaller), while more higher order intervals are observed at the same time (higher order peaks get bigger).

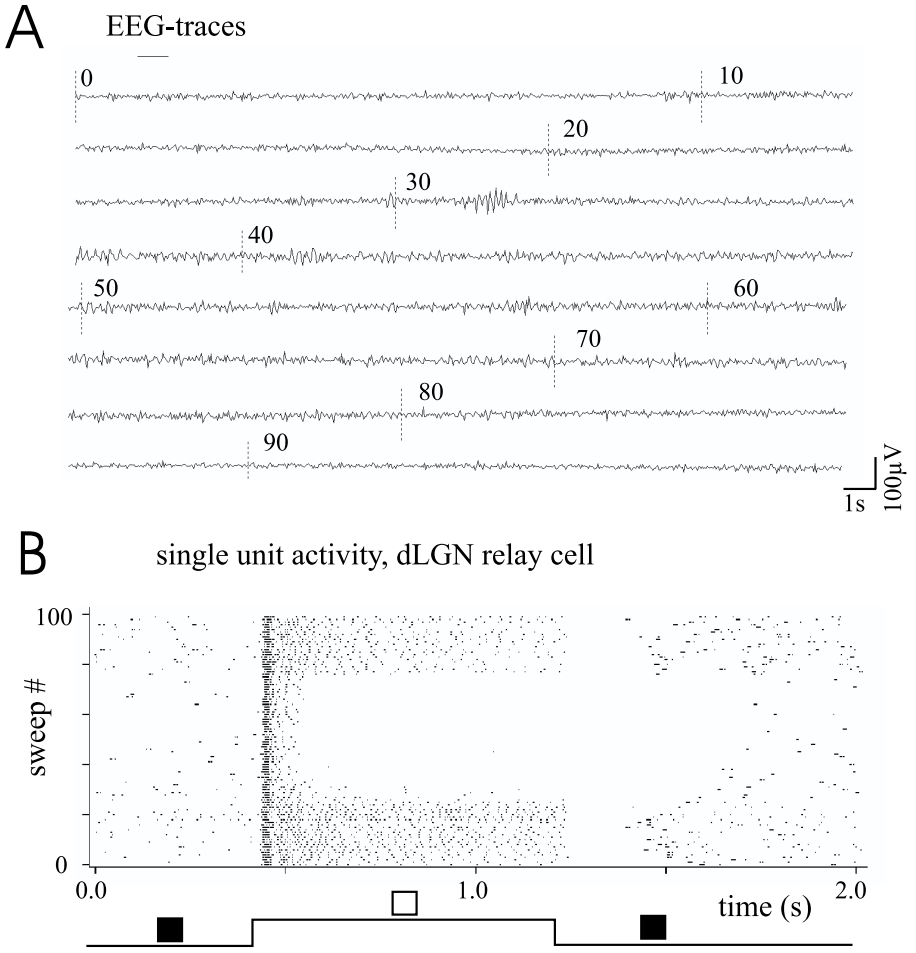

Figure 6: *Time course of the EEG-correlated change in LGN firing behavior of an X-On cell. (A) EEG-trace for 200 s of recording duration. (B) Dot raster diagram of the LGN cell recorded simultaneously with the EEG. Note the absence of the tonic visual response during the period of increased slow waves in the EEG.*

activity [21]. So far, this was found for the majority (17/18) of PGN-LGN double recordings that included a spontaneous change of the EEG pattern. Thus, the correlation between thalamic (LGN and PGN) cell behavior and EEG state is very pronounced and opposite changes in activity occur almost simultaneously. The inverse correlation between LGN and PGN activity

indicates that the PGN is strongly involved in the control of the retino-cortical transmission of visual information [21].

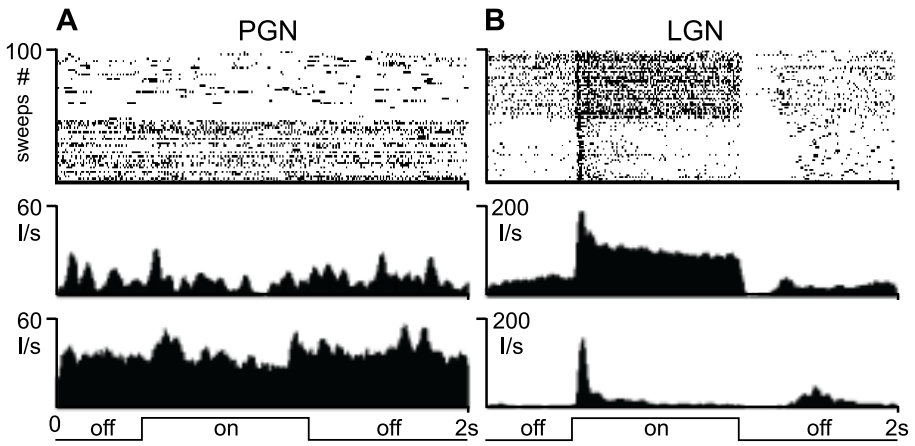

Figure 7: *LGN-PGN antagonism and its relation to the EEG. The stimulus was a small (1 deg) spot of light switched on and off within the overlapping receptive fields of the LGN and PGN cell. The PGN cell shows only a tiny visual response (A) because the stimulus was too small to efficiently stimulate the receptive field of the PGN cell. (A) PGN dot raster diagram, which shows a spontaneous transition from high tonic to burst firing around stimulus sweep 45. Two PSTHs below show the summed activity for sweeps 1-45 and 46-100, respectively. (B) Same for an LGN cell recorded simultaneously.*

The following (simplified) picture emerges [19, 21]: With high PGN activity during certain sleep states, the LGN cells will fire only phasically and a faithful transmission of stimulus properties (e.g., spatial contrast) to the cortex is largely prevented. Stimulus dependent cortical input consists mainly of brief but strong bursts of LGN activity, which are less suitable to generate a reliable visual perception but are very well suited to act as a wake-up signal [19, 27, 46]. During wakefulness, PGN activity is lower and the LGN cells will fire tonically. Stimulus properties can be encoded in the tonic firing rate

and a perceptional analysis of the visual scene becomes possible starting at the level of the primary visual cortex. It should, however, be noted that the PGN is certainly not the driving force of this process. Brain stem influences from the ascending reticular arousal system which terminate in PGN and LGN are more likely candidates for this task [2, 20, 21, 39, 41] and the complete dynamic interplay of all these structures underlies the observed activity changes.

2.4 The feed-forward influence of LGN firing onto cortical responses

Over the last years it became clear that cortical receptive fields are highly dynamic entities (for a review see [61]), which change their shape as the consequence of spatial and temporal context as well as in conjunction with the general state (of arousal or attentiveness) of the individual. In this article we will focus on two particular effects, described in the following, because these seem to directly arise from the changing afferent input activity, on which we focused so far.

2.4.1 EEG-effects on cortical cells

The strong temporal changes in the firing characteristic of LGN cells make it seem likely that their cortical targets should also display an EEG-correlated behavior. Early indications arose from the studies of Ikeda and Wright 1974 [31] who found that cortical cells respond more phasically during synchro-

nized EEG. This is probably a direct reflection of the LGN cell properties. Around 1982 a series of studies was published by a Russian group which showed that the receptive fields of cortical cells change as a reaction to an air puff (arousal stimulus) was applied to the closed eye of a paralyzed but unanesthetized animal. The stimulus applied during sleep induced a state change to a non-synchronized EEG and the cortical receptive fields, recorded while stimulating the other eye, also changed their shape [47, 55, 56, 57]. The authors attribute those receptive field changes to arousal effects mainly arising from the brain stem and also to an intracortical restructuring mechanism. The time-scale for the effects which they found was much longer (approx. 20 min) than the rather fast changes observed by us. Furthermore, a different procedure of receptive field mapping was used by these authors. In 1982, however, very little was known about the EEG-dependency of the thalamic behavior [12, 29, 37].

Fig. 8 demonstrates that cortical receptive fields change their size in an EEG-related way. These receptive field plots were measured by the "reverse correlation technique". This method determines how often any given stimulus of the applied set could have been responsible for eliciting a spike response from the cell under study [13, 14]. As stimuli we used small bright and dark dots or bars flashed with a duration of 300 ms on a medium gray background within a grid of 20x10 locations which covered the receptive field

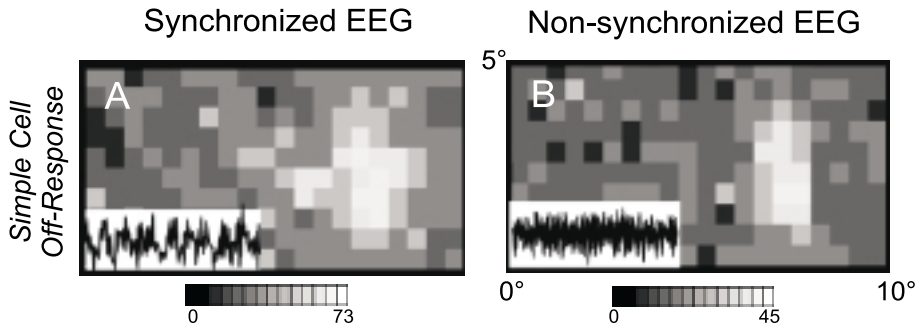

Figure 8: *State-dependent changes of receptive fields of cortical cells. Insets show EEG traces. The receptive Off-subfield of a simple cell measured during the initial part of the visual response (first 20 ms) was wider during the synchronized EEG state than during the non-synchronized state. In addition, the response was stronger as can be seen by the higher spike counts. Gray scales indicate the number of spikes counted at each grid position for a total of 30 stimulus repetitions at every position. Stimuli were short bright or dark bars (1x0.5 deg) flashed with optimal orientation in a grid of 20x10 positions corresponding to 10x5 deg of visual angle.*

completely. Furthermore, several temporal windows were predefined starting at zero delay and going back in time with equidistant steps of 10 ms. For any given spike we looked back in time and determined which stimulus location was active in the different windows. The corresponding count is raised by one and this way a 2-dimensional stimulus-response occurrence histogram is created in every time-delayed window. If, after some latency, a certain stimulus was able to elicit a spike with above-chance probability, then the corresponding bin in the latency-matched occurrence histogram stands out above noise level. This way multiple temporally staggered receptive field maps could be created which represent snapshots of the different sites and states of excitability in the region covered by the stimulus set.

The basic observation is that cortical receptive fields are larger during a synchronized EEG than during a non-synchronized EEG. This is particularly pronounced during the initial part of the response (first 20 ms, see Fig. 9) which was taken to construct the receptive field map. In a set of 63 cells we observed an average 27% increase in receptive field size that was correlated with a 2.5 fold increase in the δ-power range of the EEG [61, 64]. In control experiments we checked if the receptive fields of LGN cells also changed during a change in EEG pattern. We found, however, that they remain almost the same regardless of the EEG state. Thus, receptive field restructuring seem to be a cortical phenomenon. Novel data from our lab, however, demonstrate that these effects must be very sensitive to the level of anesthesia. The russian group [47, 55, 56, 57] used unanesthetised animals in their study and found resizing effects. However, as soon as the level of anesthesia is increased, which we did in our new set of experiments, the rf size changes are not anymore observed or can even be reverted if the activity level during the synchronized state drops to low values. A similar line of argument can be found in the studies of Edeline et al. [15] who recorded from the auditory thalamus (and cortex, personal communication) and found different effects than in our studies.

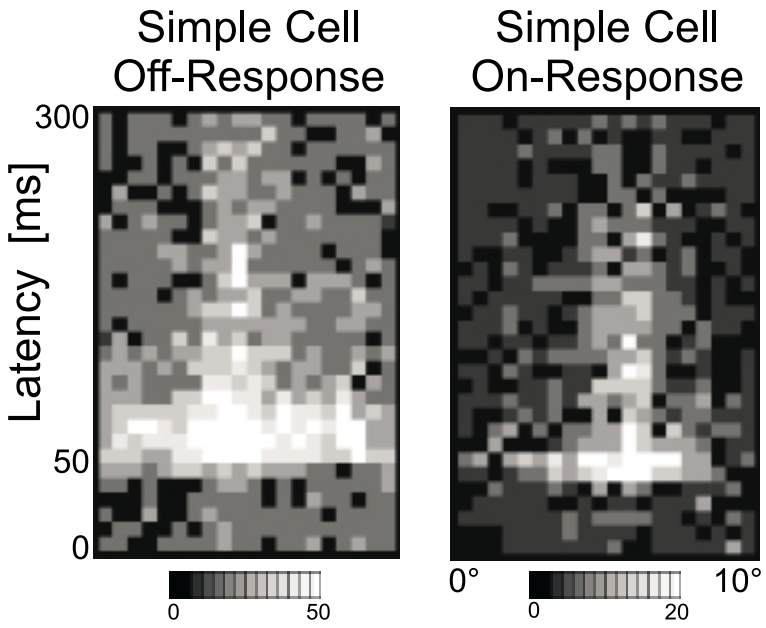

Figure 9: *Temporal changes of the size of two cortical receptive fields. The receptive fields are wide during the initial part of the visual response but considerably shrink with time when visual activity changes to a tonic response. In these diagrams only the x-dimension of the spatial receptive field plot is shown on the abscissa. Therefore, spike activity was summed up along the Y-axis of the receptive field (i.e. along the ordinate of the diagrams in figure 8). Time is plotted along the ordinate. Stimulus duration for each grid location was 300 ms.*

2.4.2 Temporal changes of cortical receptive fields

At the same time we observed that during a non-synchronized EEG the cortical receptive fields also shrink with increasing time during stimulation (Fig. 9). About fifty milliseconds after stimulation with a flashing bar the first cortical spikes can be observed. At that time responses can be elicited from a rather wide area extending into regions far laterally from the receptive field center. During the next 50 ms the receptive field shrinks and spikes cannot anymore be elicited far away from the center [64]. The shrinkage of

the receptive field can be expected to enhance the spatial resolution of the receptive field. This could in principle be accompanied with an increase of the specificity of the receptive field for certain aspects of the stimulus. However, this seems to be not the case for orientation selectivity since orientation tuning does not sharpen during the course of the visual response [10]. Other studies could not demonstrate a shrinkage of receptive field subunits because of the very short stimulus duration (40 ms) used for the mapping procedure but have shown other aspects of receptive field restructuring. For example, DeAngelis and co-workers [13] have demonstrated that the sensitivity of receptive field On- and Off-subregions can change in polarity during the course of the response.

3 Neural Field Model

In order to fit the experimental data we designed a neural field model. It is suitable not only for a qualitative, but also for a quantitative description of the experimental data. It has the advantage that it can be solved exactly and fitted to the experimental data. The analytical description furthermore allows to derive testable predictions of the dependence of model variables on experimental parameters, as for example stimulus contrast. With the help of data fitting it is possible to distinguish between different possible mechanisms of the restructuring process. In particular it can be used to determine

whether the restructuring is caused by thalamo-cortical feedforward or via intracortical feedback connections.

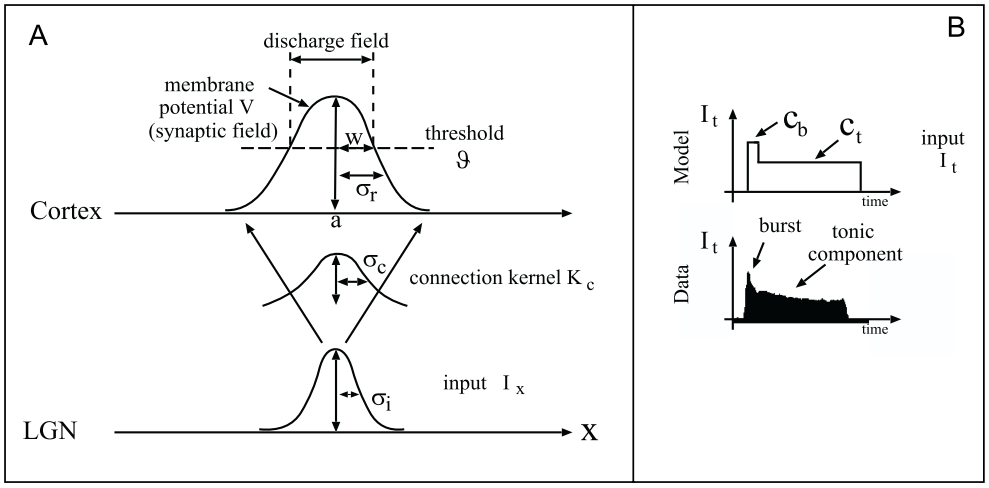

Figure 10: *Illustration of the field model and its main variables and parameters. Note, the subthreshold synaptic field width is defined by σ_r, whereas by thresholding the membrane potential with the threshold ϑ the distribution of suprathreshold, i.e. firing activity, is obtained, which equals the discharge field with half-width w.*

3.1 Theoretical Basis of the Model

In this section the neural field approach to study the LGN-V1-projection is developed. The advantage of this approach is the simplicity of the resulting model equations, which allows us to analytically compute cortical response functions for input driven activity in V1. Neural fields have been used earlier for similar purposes [26, 34, 40, 43, 59, 62].

First, we study the simplest possible field model for the description of the membrane potential distribution in the primary visual cortex: A model,

where the activity in V1 is completely determined by the LGN input $I_{lgn}(x,t)$, i.e. a pure feedforward model. Only in the next section we will compare the dynamics of the simple model with the one of a more complex model which includes intracortical feedback. Thus, we will now study membrane potential distributions, i.e. synaptic fields and not discharge fields as presented in the previous section. The discharge field can be obtained from the synaptic field applying an appropriate firing threshold.

In the model, the cortical state-variable is the mean membrane potential $V(x,t)$ of a population of neurons with similar properties located at x. Contrary to biologically realistic models, the neural activity V is assumed to be a function of the location x and not of an individual neuron, thus, V is continuous in space and time.

Just one field $V(x,t)$ is considered and intracortical feedback connections are first neglected, but included later. For convenience, we further idealize V1 as a one-dimensional field, i.e. $x \in \Re$, which is in accordance with our experimental data showing no variation in the discharge field dimension parallel to the preferred orientation [64].

The mean membrane potential V is given by a convolution of the LGN input I_{lgn} and the cortico-thalamic connection kernel K_c (Fig. 10A)

$$\tau \frac{dV(x,t)}{dt} = -V(x,t) + \int_{-\infty}^{\infty} K_c(x-x') I_{lgn}(x',t) dx' \ . \qquad (1)$$

Here, we include also a low-pass filter characterized by the phenomenological

time constant τ of the leakage term [25].

The kernel $K_c(x)$ describes the synaptic feedforward projection from LGN to cortex. We choose a Gaussian connectivity profile

$$K_c(x) = \frac{K_0}{\sqrt{2\pi}}\, e^{-\frac{x^2}{2\sigma_c^2}} \tag{2}$$

with effective synaptic strength $K_0/\sqrt{2\pi}$ and width σ_c. This profile considers the fact that the connection strength decays with distance. As the anatomical connections do not change over time in our experimental setup, they are also assumed to be constant in the model. K_c represents one single on- or off-subfield. Simple cell receptive fields consisting of several subfields can be represented by superposition of responses of the form Eqn. (1) with appropriate kernels.

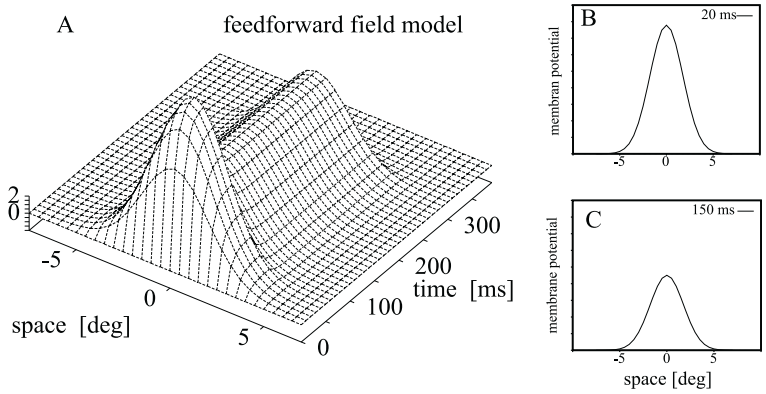

Figure 11: *A: Simulation of the cortical membrane potential $V(x,t)$ for the pure feedforward model. B, C: Time slices showing the spatial profile for the early burst phase (at 20 ms) and the late tonic phase (at 150 ms). Simulation parameters are $\sigma_c = 1.7°$, $\sigma_i = 0.5°$, $\tau = 10.0ms$, $t_0 = 0ms$, $t_1 = 40ms$, $t_2 = 300ms$, $c_b = 80I/s$, $c_t = 40I/s$.*

The synaptic input currents to V1 are fully described by the activity

of the LGN cells $I_{lgn}(x,t)$. Thereby, detailed dynamical processes in the LGN are not explicitly modeled but considered in form of phenomenological, spatio-temporally separable input functions $I(x,t) = I_x(x)I_t(t)$. The spatial input I_x has a Gaussian shape in our model, which represents a localized activity profile in the LGN (Eqn. (3)). This corresponds to the experimental stimulus in form of a small light spot. As we did not see any changes of the spatial activity profile in the experimental LGN data, the assumption of a constant σ_i seems justified. The temporal input component I_t approximates the experimentally observed temporal firing patterns of LGN cells (Fig. 10B).

$$I_x(x) = e^{-\frac{x^2}{2\sigma_i^2}} \tag{3}$$

$$I_t(t) = c_b\Theta(t-t_0)\Theta(t_1-t) + c_t\Theta(t-t_1)\Theta(t_2-t)\ . \tag{4}$$

The function $I_t(t)$ describes the thalamic firing response with an initial high-frequency burst response—modeled in form of a rectangular pulse of strength c_b lasting from $t = t_0$ to t_1—followed by the tonic component of height $c_t (< c_b)$ lasting from t_1 to t_2 (Fig. 10B). $\Theta(t)$ is the Heaviside function. A further assumption of the model is that the activities in V1 are also spatio-temporally separable, i.e. $V(x,t) = X(x)T(t)$ (see [13, 40]).

Figure 11 shows a simulation of the model. The cortical membrane potential V is plotted as a function of space and time (A). In accordance with the experimental data (cf. Figs. 8,9) a phasic peak is followed by a tonic component with a reduced amplitude. This restructuring from early phasic to

late tonic component can clearly be seen by looking at time slices (B vs. C).

3.2 Neural Field Model with Intracortical Feedback

The analyzed feedforward model is a reduced model since in reality there also exist massive cortico-thalamic and intracortical feedback connections. Therefore, it is necessary to compare the dynamics of the pure feedforward model with the dynamics of a model including also feedback connections by adding a cortical loop to the simple feedforward model:

$$\tau \frac{\partial V(x,t)}{\partial t} = -V(x,t) + X(x) I_t(t) + \int_{-\infty}^{\infty} K_{DOG}(x-x') R(V(x',t))\, dx' \ . \quad (5)$$

The cortical connection kernel K_{DOG} is chosen as a difference of Gaussians to include excitatory feedback for short and inhibitory feedback for long distances

$$K_{DOG}(x) = \frac{K_{exc}}{\sqrt{2\pi}} e^{-\frac{x^2}{2\sigma_{exc}^2}} - \frac{K_{inh}}{\sqrt{2\pi}} e^{-\frac{x^2}{2\sigma_{inh}^2}} \ . \quad (6)$$

Parameters are such that K_{DOG} has a Mexican hat profile. The rate function $R(V)$ in Eqn. (5) is zero for $V \leq 0$ and equal to βV for $V > 0$. β is the neuronal gain (in spikes/s/mV). Input from LGN is the same as in the feedforward model. Note, however, that in Eqn. (5) we have already inserted the total spatial input $X(x)$ into cortex, that is, the spatial convolution of the LGN activity $I_x(x)$, Eqn. (3), and the feedforward kernel from LGN to cortex, Eqn. (2). The temporal input component I_t in Eqn. (5) is given by

Eqn. (4). Similar models have been investigated recently in the context of orientation tuning in V1 [1, 4, 8].

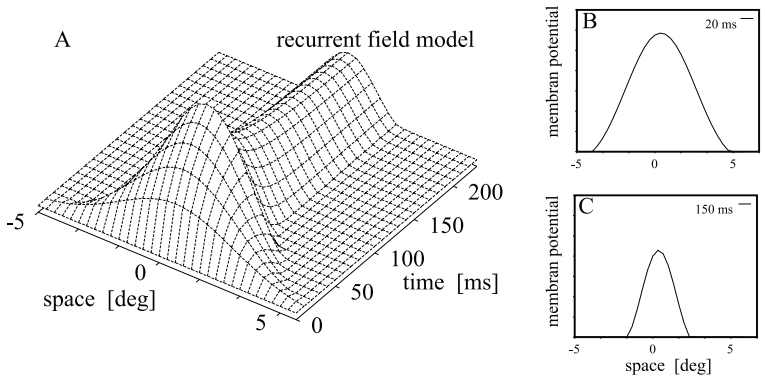

Figure 12: *A: Simulation of the cortical membrane potential including intracortical feedback. B,C: Time slices showing the spatial profile for the early burst phase (at 20 ms) and the late tonic phase (at 150 ms). Compared to the feedforward model (Fig. 11) the spatial profile significantly changes over time in the feedback model.*

Due to the non-linear feedback connections, analytic solutions of Eqn. (5) cannot be given. Therefore, we simulate Eqn. (5) and discuss the qualitative differences that appear in contrast to the simple feedforward model. As parameters, we choose $\tau = 10ms$, $t_0 = 0ms$, $t_1 = 50ms$, $t_2 = 300ms$ and (somewhat arbitrarily) $\sigma_r = 3°$, $\sigma_{exc} = 0.7°$, $\sigma_{inh} = 3.0°$, $K_{exc}\beta = 2.0mV/deg$, and $K_{inh}\beta = 0.5mV/deg$. Furthermore, we define $k := K_0\sigma_c\sigma_i/\sigma_r$, $C_1 = kc_b$, $C_2 = kc_t$ and choose the effective cortical inputs $C_1 = 10mV$ and $C_2 = 2.5mV$ for the burst and the tonic phase.

With these parameters the network operates in a regime of cortical amplification, as it has been proposed for recurrent orientation tuning models [1, 4, 8, 51]. Thereby, the model behavior is constant within a wide range of

parameters and does not depend on the exact values.

At a first glance, the membrane potential $V(x,t)$ of the recurrent model as shown in Fig. 12 A looks similar to the one of the feedforward model (Fig. 11): Again a strong and wide component dominates during the first 50 ms and is followed by a weaker and smaller tonic component. There is nonetheless a subtle but important difference described in the next subsection.

3.2.1 Cortical Membrane Potential and Width of the Discharge Field

For the pure feedforward model, the membrane potential cannot only be simulated as shown in Fig. 11 but also derived analytically. The equations can be found in [54]; in the context of this review we will restrict ourselves to a diagram which shows the main finding. The same will be shown for the model with feedback, where an analytical derivation is not possible and we had, from the beginning, to resort to a numerical solution.

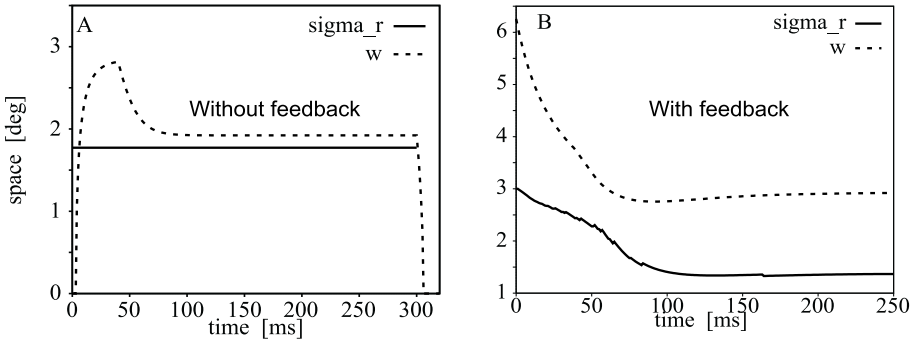

Figure 13: *Size of the synaptic field and the discharge field for the model without (A) and with (B) feedback. The synaptic field σ_r remains constant when no feedback is present.*

In Fig. 13 we plot the receptive field width w and the width of the synaptic field σ against time. The synaptic field width is identical to the width of the subthreshold membrane potential (at half-height above baseline). The receptive field width is obtained by applying a ("firing") threshold to the synaptic field.

We observe as a major model result that in a pure feedforward model the width σ_r of the subthreshold cortical synaptic field is constant over time (Fig. 13A), whereas σ_r gets smaller over time in the model with feedback (Fig. 13B). The width w of the suprathreshold discharge field shrinks in both cases.

Strictly speaking the width σ is not well defined in the recurrent model, because the potential profile is no longer Gaussian. We can, however, still fit the central peak of the profile to a Gaussian function to obtain an effective width, $\sigma(t)$, which was used to generate the plot in Fig. 13B using the result from Fig. 12.

The model analysis can be extended to more spatial and temporal parameters and other testable predictions arise (see [54]). This, however, exceeds the scope of this review article.

3.3 Results of the Model Fit to the Data

In order to test the validity of our major model results stated above, a fitting procedure to the experimental data is carried out (details of the standard

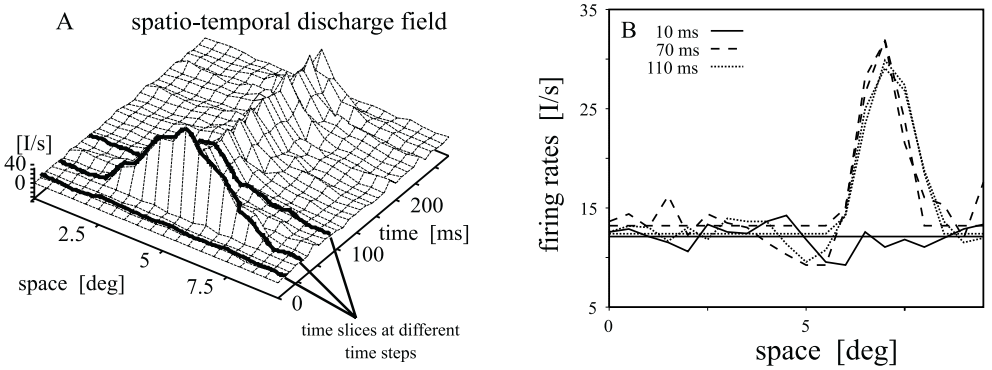

Figure 14: *A: Illustration of the data fit. The diagram in A is similar to the gray scale plot shown in Fig. 9 only here we plot it in 3-D in order to better show the data fitting quality for thirty cross-section (every 10 ms) which are fit. B: Original data and fit of a cortical simple cell (on-field) to the spatial activity $q(t_i)X(x)$ for three selected time slices t_i. As the stimulus response does not start before approximately 50 ms in the examples shown, the data at 10 ms gives an impression of the background noise contained in the data, fitted by a constant value. The activity declines with progressing time (70 to 110 ms).*

fitting procedure can again be found in [54]. Here we only show one example out of 38 to demonstrate the quality of the fit (Fig. 14). From the fitting procedure the parameters w and σ can be extracted from the experimental data and compared against the theoretical predictions.

3.3.1 Width σ is constant over time

Figs. 15 shows the width of the cortical synaptic field plotted as a function of time for one example neuron. After the activity has reached V1 (around $t_0 = 40$ ms), σ turns out to be constant over time. This was the case in almost all sampled subfields. Only two subfields revealed slight and insignificant trends towards larger values of σ with increasing time.

Receptive fields in experiments are most commonly derived from firing rates and not from intracellular potentials. As a measure for the width of the discharge field we choose its half-width w (Fig. 15). This can be compared to the width σ of the synaptic field and it is computable from the fitted model parameters. Clearly, w is time dependent even though σ is not (Fig. 15). This shows that the pure feed-forward model suffices to explain the effect of temporal shrinking of cortical receptive fields.

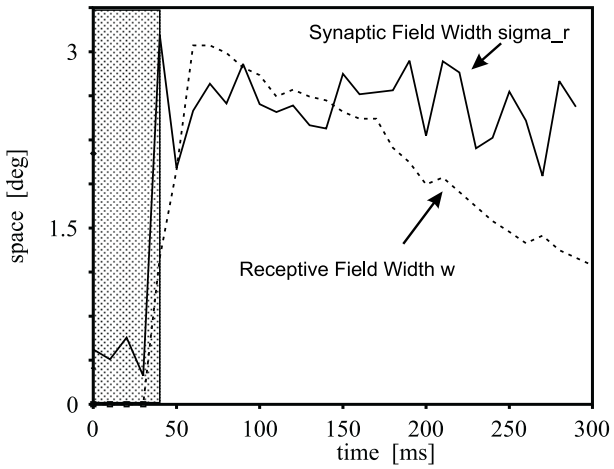

Figure 15: *Time course of the synaptic and the receptive field width model parameters obtained from the spatial fit. Note that the LGN activity does not reach V1 before approximately 40 ms (grey areas); up to that time background noise is fitted and the resulting fit parameters are meaningless.*

4 Conclusion

In this article we have tried to provide an overview about the spatial and temporal response properties of LGN cells and about their direct influence on visual cortical cells. In particular the last decade has shown that the

anatomical structure and the responses found in the LGN have a much higher complexity than originally expected from a "mere" relay nucleus. The thalamus plays a major role not only in relaying primary afferent activity to the cortex, but also on controlling the sleep-waking pattern and probably even on the generation of early cognitive properties, like pop-out phenomena or pre-attentive gating (for a review see [53]). While it took some time before these more complex actions of the thalamus were acknowledged, it was from the beginning clear that the thalamus is the gateway for the primary afferent signal flow in all sensory systems (except olfaction). However, in the visual system even this apparently so simple action immediately leads to elaborate spatio-temporal response pattern in the cortical target cells. Quite obviously the cortical network adds a significant degree of complexity to the cell behavior, however, the reported findings show that already the feedforward action of the afferent input is able to alter the shape of the receptive field of their its cortical targets.

References

[1] Adorjan, P., Levitt, J., Lund, J. & Obermayer, K. (1999). A model for the intracortical origin of orientation preference and tuning in macaque striate cortex. *Vis. Neurosci.* **16**, 303-18.

[2] Ahlsn, G. & Lo, F.-S. (1982) Projection of brainstem neurons to the peri-

geniculate nucleus and the lateral geniculate nucleus in the cat. *Brain Res.*, **238**, 433-438.

[3] Bal, T., von Krosigk, M., & McCormick, D.A. (1995) Role of the ferret perigeniculate nucleus in the generation of synchronized oscillations in vitro. *J. Physiol.*, **483**, 665-685.

[4] Ben-Yishai R., Baror R.L., & Sompolinsky H. (1995) Theory of orientation tuning in visual cortex. *Proc. Natl. Acad. Sci. USA*, **92**, 3844-3848.

[5] Bolz, J., Rosner, G. & Wässle, H. (1982) Response latency of brisk-sustained (X) and brisk-transient (Y) cells in the cat retina. *J. Physiol.* **328**, 171-190.

[6] Bullier, J. & Norton, T.T. (1979) Comparison of receptive-field properties of X and Y ganglion cells with X and Y lateral geniculate cells in the cat. *J. Neurophysiol.* **42**, 274-291.

[7] Burke, W., & Cole, A.M. (1978) Extraretinal influences on the lateral geniculate nucleus. *Rev. Physiol. Biochem. Pharmacol.*, **80**, 105-180.

[8] Carandini, M. & D. Ringach (1997). Predictions of a recurrent model of orientation selectivity. *Vision Res.* **37**, 3061-3071.

[9] Casagrande, V.A. & Norton, T.T. (1991) The lateral geniculate nucleus:a review of its physiology and function. In: *The Neural Basis of Visual Function* 4:41-84.

[10] Celebrini, S., Thorpe, S., Trotter, Y. & Imbert, M. (1993) Dynamics of orientation coding in area V1 of the awake primate. *Vis. Neurosci.*, **10**, 811-825.

[11] Cleland, B.G., Dubin, M.W. & Levick, W.R. (1971) Sustained and transient neurones in the cat's retina and lateral geniculate nucleus. *J. Physiol.* **217**, 473-496.

[12] Coenen, A.M.L., & Vendrick, A.J.H. (1972) Determination of the transfer ratio of cats geniculate neurons through quasi-intracellular recordings and the relation with the level of alertness. *Exp. Brain Res.*, **14**, 227-242.

[13] DeAngelis, G., Ohzawa, I., & Freeman, R. (1995) Receptive-field dynamics in the central visual pathway. *TINS*, **18**, 451-458.

[14] Eckhorn, R., Krause, F., & Nelson, J.J. (1993) The RF-cinematogram. A cross-correlation technique for mapping several visual receptive fields at once. *Biol. Cybern.*, **69**, 37-55.

[15] Edeline, J.-M., Manunta, Y. & Hennevin, E. (2000). Auditory thalamus neurons during sleep: Changes in frequency selectivity, threshold and receptive field size. *J. Neurophysiol.*, **84**, 934-952.

[16] Enroth-Cugell, C. & Lennie, P. (1975) The control of retinal ganglion cell discharge by receptive field surrounds. *J. Physiol.* **247**, 551-578.

[17] Eysel, U.T. (1986) Spezifische Leistungen thalamischer Hemmungsmechanismen im Sehsystem. *Physiologie Aktuell*, **2**, 159-175.

[18] Fischer, B. & Krüger, J. (1974) The shift-effect in the cat's lateral geniculate neurons. *Exp. Brain Res.*, **21**, 225-227.

[19] Funke, K. & Eysel, U.T. (1992) EEG-dependent modulation of response dynamics of cat dLGN relay cells and the contribution of corticogeniculate feedback. *Brain Res.*, **573**, 217-227.

[20] Funke, K., & Eysel, U.T. (1993) Modulatory effects of acetylcholine, serotonin and noradrenaline on the activity of cat perigeniculate neurons. *Exp. Brain Res.*, **95**, 409-420.

[21] Funke, K. & Eysel, U. (1998) Inverse correlation of firing patterns of single topographically matched perigeniculate neurons and cat dorsal lateral geniculate relay. *Vis. Neurosci.*, *15*, 711-729.

[22] Funke, K. & Wörgötter, F. (1995) Temporal structure in the light response of relay cells in the dorsal lateral geniculate nucleus of the cat. *J. Physiol.*, **485**, 715-737.

[23] Funke, K. & Wörgötter, F. (1997) On the significance of temporally structured activity in the dorsal lateral geniculate nucleus (LGN). *Prog. Neurobiol.* **53**, 67-119.

[24] Gaudiano, P. (1994) Simulations of X and Y retinal ganglion cell behavior with a nonlinear push-pull model of spatiotemporal retinal processing. *Vision Res.* **34**, 1767-1784.

[25] Gerstner, W. (1998). Spiking neurons. In: *Pulsed Neural Networks.*, W. Maass and C. M. Bishop (Eds.), MIT press.

[26] Giese, M. A. (1999). Dynamic neural field theory for motion perception. Massachusetts: Kluwer Academic.

[27] Guido, W. & Weyand, T. (1995) Burst responses in thalamic relay cells of the awake, behaving cat. *J. Neurophysiol.*, **74**, 1782-1786.

[28] Heggelund, P., Karlsen, H.E., Flugsrud, G. & Nordtug, T. (1989) Response to rates of luminance change of sustained and transient cells in the cat lateral geniculate nucleus and optic tract. *Exp. Brain Res.* **74**, 116-130.

[29] Hirsch, J.C., Fourment, A., & Marc, M.E. (1983) Sleep-related variation of membrane potential in the lateral geniculate body relay neurons of the cat. *Brain Res.* **259**, 308-312.

[30] Hubel, D.H. & Wiesel, T.N. (1961) Integrative action in the cat's lateral geniculate body. *J. Physiol.* **155**, 385-398.

[31] Ikeda, H. & Wright, M. (1974) Sensitivity of neurones in visual cortex (area 17) under different levels of anaesthesia. *Exp. Brain Res.*, **20**, 471-484.

[32] Kaplan, E., Mukherjee, P. & Shapley, R. (1993) Information filtering in the lateral geniculate nucleus. In: *Contrast Sensitivity*, Vol. 5, 183-200.

[33] Kim, U., Bal, T. & McCormick, D.A. (1995) Spindle waves are propagating synchronized oscillations in the ferret LGNd in vitro. *J. Neurophysiol.*, **74**, 1301-1323.

[34] Krone, G., Mallot, H.P., Palm, G. & Schüz, A. (1986). Spatiotemporal receptive fields: a dynamical model derived from cortical architectonics. *Proc. Roy. Soc. (Lond.)*, **226**, 421-444.

[35] Kuffler, S.T.W. (1953) Discharge patterns and functional organization of mammalian retina. *J. Neurophysiol.* **16**, 37-68.

[36] Li, B., Funke, K., Wörgötter, F. & Eysel, U.T. (1999) Correlated variations in EEG pattern and visual responsiveness of cat lateral geniculate relay cells. *J. Physiol.*, **514**, 857-874.

[37] McCarley, R.W., Benoit, O., & Barrionuevo, G. (1983) Lateral geniculate nucleus unitary discharges in sleep and waking: State- and rate-specific aspects. *J. Neurophysiol.*, **50**, 798-818.

[38] McCormick, D.A. (1992) Neurotransmitter actions in the thalamus and cerebral cortex and their role in neuromodulation of thalamocortical activity. *Prog. Neurobiol.*, **39**, 337-388.

[39] McCormick, D.A., & Bal, T. (1997) Sleep and arousal: Thalamocortical mechanisms. *Ann. Rev. Neurosci.*, **20**, 185-215.

[40] Mineiro, P. & Zipser, D. (1998). Analysis of direction selectivity arising from recurrent cortical interactions. *Neural Comp.* **10**, 353-371.

[41] Murphy, P., Uhlrich, D., Tamamaki, N., & Sherman, S. (1994) Brainstem modulation of the response properties of cells in the cats perigeniculate nucleus. *Vis. Neurosci.*, **11**, 781-791.

[42] Rodieck, R.W. & Stone, J. (1965) Analysis of receptive fields of cat retinal ganglion cells. *J. Neurophysiol.* **28**, 833-849.

[43] Sabatini, S. P. & Solari, F. (1999). An architectural hypothesis of direction selectivity in the visual cortex: the role of spatially asymmetric intracortical inhibition. *Biol. Cybern.* **80**, 171-183.

[44] Sanchez-Vives, M. & McCormick, D.A. (1997) Functional properties of perigeniculate inhibition of dorsal lateral geniculate nucleus thalamocortical neurons in vitro. *J. Neurosci.*, **17**, 8880-8893.

[45] Shapley, R. & Hochstein, S. (1975) Visual spatial summation in two classes of geniculate cells. *Nature* **256**, 411-413.

[46] Sherman, S. & Koch, C. (1990) Thalamus. In: *The Synaptic Organization of the Brain*, Shepherd, G. (Ed)., Oxford University Press, New York, 3rd edition, 246-278.

[47] Shevelev, I., Sharaev, G., Voglushev, M., Pyshnyi, M., & Verderevskaia, N. Dynamics of the receptive fields of visual cortex and lateral geniculate body neurons in the cat. *Neirofiziologiia*, **14**, 622-630, (in Russian).

[48] Singer, W. (1977) Control of thalamic transmission by corticofugal and ascending pathways in the visual system. *Physiol. Rev.* **57**, 386-420.

[49] Singer, W. & Creutzfeldt, O.D. (1970) Reciprocal lateral inhibition of On- and Off-center neurones in the lateral geniculate body of the cat. *Exp. Brain Res.* **10**, 311-330.

[50] Singer, W., Pöppel, E. & Creutzfeldt, O. (1972) Inhibitory interaction in the cat's lateral geniculate nucleus. *Exp. Brain Res.* **14**, 210-226.

[51] Somers, D. C., Nelson, S.B., & Sur, M. (1995). An emergent model of orientation selectivity in cat visual cortical simple cells. *J. Neurosci.* **15**, 5465-5488.

[52] Steriade, M., McCormick, D., & Sejnowski, T. (1993) Thalamocortical oscillations in the sleeping and aroused brain. *Science*, **262**, 679-685.

[53] Suder, K. & Wörgötter, F. (2000) The control of low-level information flow in the visual system. *Rev. Neurosci.*, **11**, 127-146.

[54] Suder, K., Wörgötter, F. & Wennekers, T. (2000) Neural field model of receptive field restructuring in primary visual cortex. *Neural Comp.*, **13**, Nov. 2000 in press.

[55] Verderevskaia, N. & Shevelev, I. (1979) Relationship between level of vigilance and changes in the receptive fields of the cat visual cortex. *Zh. Vyssh. Nerv. Deiat.*, **29(5)**, 1001-1008, (in Russian).

[56] Verderevskaya, N. & Shevelev, I. (1981) Change in the receptive fields of the visual cortex of the cat in the relation to the level of wakefulness. *Neurosci. Behav. Physiol.*, **11(6)**, 563-569.

[57] Verderevskaya, N. & Shevelev, I. (1982) Receptive fields of neurons in the cat's visual cortex after a change of alertness level. *Acta Neurobiol. Exp. Warsz.*, **42**, 75-91.

[58] Wang, X.J. & Rinzel, J. (1993) Spindle rhythmicity in the reticularis thalami nucleus: synchronization among mutually inhibitory neurons. *Neurosci.*, **53**, 899-904.

[59] Wilson, H. R. & Cowan, J.D. (1973). A mathematical theory of the functional dynamics of cortical and thalamic nervous tissue. *Kybernetik*, **13**, 55-80.

[60] Wilson, J.R. (1993) Circuitry of the dorsal lateral geniculate nucleus in the cat and monkey. *Acta Anat.*, **147**, 1-13.

[61] Wörgötter F & Eysel, U.T. (2000) Context, state and the receptive field of striatal cortical cells. *TINS*, **23**, 497-503.

[62] Wörgötter F, Niebur, E. & Koch, C. (1991). Isotropic connections generate functional asymmetrical behavior in visual cortical cells. *J. Neurophysiol.*, **66**, 444-459.

[63] Wörgötter, F., Suder, K. & Funke, K. (1999). The dynamic spatio-temporal behavior of visual responses in thalamus and cortex. *Restor. Neurol & Neurosci.* **15**, 137-452.

[64] Wörgötter, F., Suder, K., Zhao, Y., Kerscher, N., Eysel, U., & Funke, K. (1998) State-dependent receptive field restructuring in the visual cortex. *Nature*, **396**, 165-168.